Perturbation and Predissociation near the Dissociation Limit of the $B^1\Pi$ State of $^{23}Na^{39}K$

Shunji Kasahara, Masaharu Shibata, Masaaki Baba,† and Hajime Katô*

Department of Chemistry, Faculty of Science, Kobe University, Nada-ku, Kobe 657, Japan

Received: June 5, 1996; In Final Form: August 5, 1996[⊗]

The J' dependencies of energy and line width of the $^{23}Na^{39}K$ $B^1\Pi(v' = 30-43, J') \leftarrow X^1\Sigma^+(v'' = 2, J'')$ transitions are measured up to the breaking-off points, where NaK dissociates to the $Na(3s^2S_{1/2}) + K(4p^2P_{3/2})$ atoms. Line broadenings are observed for transitions to the $B^1\Pi(v' = 30, J' \geq 42)$, $(v' = 31, J' \geq 35)$, $(v' = 32, J' \geq 27)$, $(v' = 33, J' \geq 14)$, and $(v' \geq 34$, all $J')$ levels, and are attributed to the predissociation via the $c^3\Sigma^+$ state to the $Na(3s^2S_{1/2}) + K(4p^2P_{1/2})$ atoms. The (v', J') dependence of the predissociation threshold is attributed to the potential barrier due to rotation. Below and near the threshold, a series of the perturbation centers which converge to the predissociation threshold is observed for each v', and the perturbing state is identified as the $c^3\Sigma^+$ state. Rotational perturbations are observed also above the predissociation threshold, and the perturbing state is identified as the $b^3\Pi_1$ state. The line widths are observed to change drastically around the maximum perturbation, and this is identified as originating from the interference effect which arises because both the $B^1\Pi$ and $b^3\Pi_1$ states interact with the dissociative continuum of the $c^3\Sigma^+$ state. In the transitions to levels near the breaking-off points of the $B^1\Pi(v' \geq 37)$, the line splittings into two lines are observed for each J'. This splitting is identified as originating from the *S*-uncoupling interaction between the $B^1\Pi$ and $b^3\Pi$ states at a long internuclear distance. Similar line splittings are observed for the $B^1\Pi(v' = 30$, all $J')$ levels, but are not observed for $v' = 31-36$. An accidental coincidence of the level energies of the $B^1\Pi(v' = 30)$ and $b^3\Pi(v)$ levels is presumed, and the origin of the line splitting is identified as the *S*-uncoupling interaction. This is confirmed by the analysis of the hyperfine structures observed for the split lines.

Introduction

The $B^1\Pi$ state of the NaK molecule is correlated with the separated atoms $Na(3s^2S_{1/2}) + K(4p^2P_{3/2})$. The level energies of the $K(4p^2P_{3/2})$ and $K(4p^2P_{1/2})$ atoms are, respectively, 13 042.89 and 12 985.17 cm^{-1}.[1] In our previous report,[2] Doppler-free high-resolution spectra of the $B^1\Pi(v', J' = 16$ and $18) \leftarrow X^1\Sigma^+(v'' = 4, J'' = 17)$ transitions up to $v' = 43$ were measured by the technique of optical−optical double resonance polarization spectroscopy (OODRPS).[3−5] Remarkable line broadenings were observed for transitions higher than the dissociation energy to $Na(3s^2S_{1/2}) + K(4p^2P_{1/2})$ atoms, and the broadenings were identified as originating from the predissociation to $Na(3s^2S_{1/2}) + K(4p^2P_{1/2})$ atoms. The predissociation was shown to be caused by the spin−orbit interaction between the $B^1\Pi$ and $c^3\Sigma^+$ states. However, only two rotational levels for each v', $B^1\Pi(v', J' = 16$ and $18)$, were measured in ref 2. We extended the study and obtained data over a wider range of the rotational quantum number J', and the results are reported in this article.

At short internuclear distance, there are four molecular states $B^1\Pi$, $A^1\Sigma^+$, $b^3\Pi$, and $c^3\Sigma^+$ correlated with the separated atoms $Na(3s^2S) + K(4p^2P)$. The potential energy curves[2,6−8] calculated by the Rydberg−Klein−Rees (RKR) method[9,10] are shown in Figure 1A. Only the curve of the $c^3\Sigma^+$ state crosses with the one of the $B^1\Pi$ state at the inner part, where the $B^1\Pi$ and $c^3\Sigma^+$ states are mixed by the spin−orbit interaction.

At long internuclear distance, the effect of the spin−orbit interaction becomes significant, and the electronic states transform into Hund's case c. The energies and eigenfunctions for a given internucler distance R (>8 Å) were calculated by diagonalizing the energy matrix composed of long-range potential energies and the spin−orbit interaction, and the results

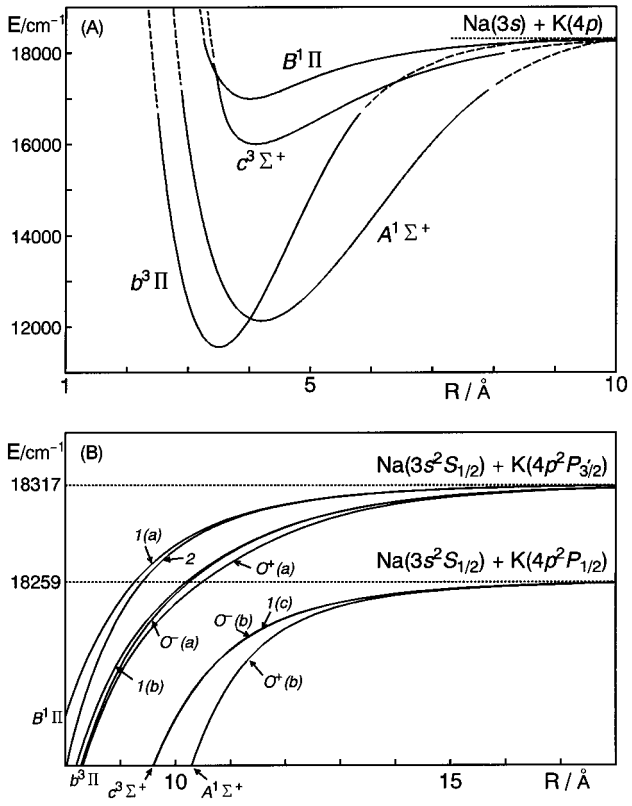

Figure 1. Potential energy curves of states derived from the Na(3s) + K(4p) atoms. The upper trace is the RKR potentials calculated from the molecular constants reported in Table 1 for $B^1\Pi$, in ref 6 for $A^1\Sigma^+$, in ref 8 for $c^3\Sigma^+$, and in ref 7 for $b^3\Pi$ states (full lines; the extrapolated parts are shown by broken lines). The lower trace is the potential curves at long internuclear distance, which are calculated by including the spin−orbit interaction (see ref 2).

† Present address: Faculty of Integrated Human Studies, Kyoto University, Sakyo-ku, Kyoto 606, Japan.

⊗ Abstract published in *Advance ACS Abstracts,* December 15, 1996.

S1089-5639(96)01631-3 CCC: $14.00

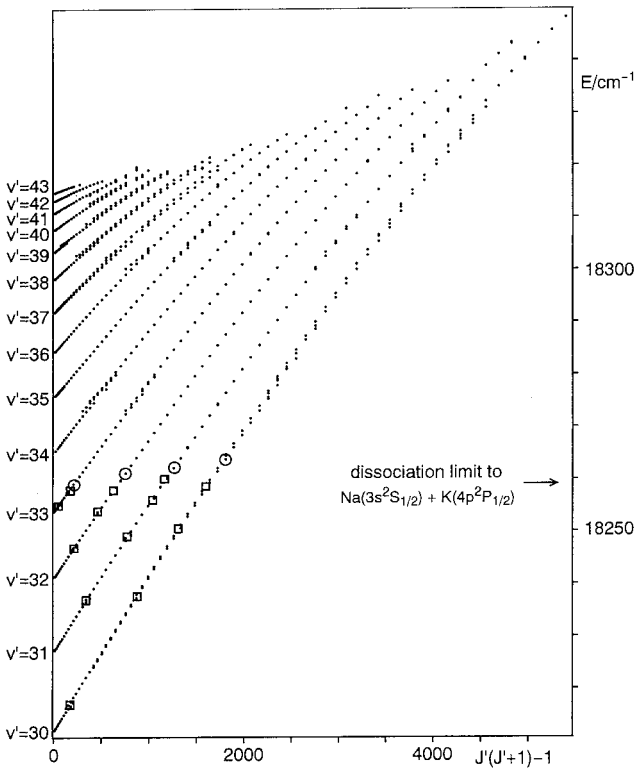

Figure 2. Term values of the observed levels are plotted against $J'(J'+1)-1$. The line broadenings are observed for all rotational levels of $v' > 34$ and rotational levels larger than J'_b for $v' \leq 33$. The levels of J'_b for $v' \leq 33$ are shown by open circles, which indicate the predissociation thresholds. The energy of the dissociation limit to the separated atoms $Na(3s^2S_{1/2}) + K(4p^2P_{1/2})$ is shown by an arrow. The perturbation centers which converge to the predissociation threshold are shown by open squares.

at various R were reported in ref 2 (the potential curves are shown in Figure 1B). The outer part of the RKR potential of the $B^1\Pi$ state converges to the potential curve of the 1(a) state. The $^1\Pi(\Omega = \pm 1)$ state mixes with the $^3\Pi(\Omega = \pm 1)$ and $^3\Sigma^+(\Omega = \pm 1)$ states by the spin−orbit interaction, and the resulting eigenfunctions were listed in Table V of ref 2.

Results and Discussion

We used a technique of the Doppler-free OODRPS, and the experimental arrangements were the same as in our previous report.[11] It was estimated from the potential curves of the $B^1\Pi$ and $X^1\Sigma^+$ states[2,12] that the levels near the dissociation limit of the $B^1\Pi$ state could be excited from the $X^1\Sigma^+(v'' = 2, J'')$ levels. A pump laser beam was fixed to the center of Doppler-free line of a known transition $B^1\Pi(v' = 1, J''+1$ or J'' or $J''-1) \leftarrow X^1\Sigma^+(v'' = 2, J'')$ of $^{23}Na^{39}K$ and was modulated by a chopper. Then, we scanned the probe laser and observed the $B^1\Pi(v', J'' \pm 1$ or $J'') \leftarrow X^1\Sigma^+(v'' = 2, J'')$ transitions of v' from 30 to above the breaking-off point, where the spectrum became diffuse and no spectral line was observed. The J'' was changed successively, and the J' dependencies of the energy and line width of the $B^1\Pi(v', J') \leftarrow X^1\Sigma^+(v'' = 2, J'')$ transition for $v' = 30-43$ were observed. The term value of the observed level, which is obtained by adding the energy of the $X^1\Sigma^+(v'' = 2, J'')$ level to the observed transition energy, is plotted against $J'(J'+1) - 1$ in Figure 2. A number of J' levels at each v' were observed to be perturbed: energy shifts from the extrapolated line positions and/or line broadenings or hyperfine splittings were observed. Molecular constants are determined by a least-squares fitting for all observed rotational levels of each v' without throwing out perturbed levels, and the results are listed in Table 1.

TABLE 1: Molecular Constants T_v, B_v, D_v, and H_v for $v = 30-43$ of the $^{23}Na^{39}K$ $B^1\Pi$ State (All Values in Units of cm^{-1})

v	T_v	10^2B_v	10^6D_v	$10^{10}H_v$
30	18 211.803	3.028 65	−0.575 11	−0.647 25
31	18 227.047	2.888 03	−0.650 39	−0.718 81
32	18 241.113	2.720 85	−0.556 27	−1.173 72
33	18 253.815	2.562 92	−0.566 58	−1.502 94
34	18 265.204	2.441 98	−1.005 09	−0.946 45
35	18 275.788	2.136 85	−0.057 04	−3.440 30
36	18 284.198	2.124 85	−1.325 65	−1.479 82
37	18 291.798	1.914 30	−1.868 13	0.905 63
38	18 298.140	1.790 69	−2.424 98	0.485 03
39	18 303.452	1.573 78	−2.083 44	−2.412 65
40	18 307.562	1.424 41	−3.840 69	10.415 21
41	18 310.795	1.213 23	−6.878 68	52.535 05
42	18 313.162	0.930 48	−2.334 57	−7.231 57
43	18 314.760	0.731 68	−1.084 90	−63.197 45

At long internuclear distance, the $B^1\Pi$, $A^1\Sigma^+$, $b^3\Pi$, and $c^3\Sigma^+$ states are strongly mixed by the spin−orbit interaction. The wave functions of the $^1\Pi$, $^3\Pi$, $^1\Sigma^+$, and $^3\Sigma^+$ states in Hund's case a are given by[13]

$$|^1\Pi \pm vJM\rangle = (1/\sqrt{2})(|1\rangle|00\rangle|v\rangle|J1M\rangle \pm |-1\rangle|00\rangle|v\rangle|J-1M\rangle) \quad (1)$$

$$|^3\Pi_2 \pm vJM\rangle = (1/\sqrt{2})(|1\rangle|11\rangle|v\rangle|J2M\rangle \pm |-1\rangle|1-1\rangle|v\rangle|J-2M\rangle)$$

$$|^3\Pi_1 \pm vJM\rangle = (1/\sqrt{2})(|1\rangle|10\rangle|v\rangle|J1M\rangle \pm |-1\rangle|10\rangle|v\rangle|J-1M\rangle)$$

$$|^3\Pi_0 \pm vJM\rangle = (1/\sqrt{2})(|1\rangle|1-1\rangle|v\rangle|J0M\rangle \pm |-1\rangle|11\rangle|v\rangle|J0M\rangle) \quad (2)$$

$$|^1\Sigma^+_{0^+}vJM\rangle = |0^+\rangle|00\rangle|v\rangle|J0M\rangle \quad (3)$$

$$|^3\Sigma^+_1 \pm vJM\rangle = (1/\sqrt{2})(|0^+\rangle|11\rangle|v\rangle|J1M\rangle \pm |0^+\rangle|1-1\rangle|v\rangle|J-1M\rangle)$$

$$|^3\Sigma^+_{0^-}vJM\rangle = |0^+\rangle|10\rangle|v\rangle|J0M\rangle \quad (4)$$

where the basis function is expressed as $|\Lambda\rangle|S\Sigma\rangle|v\rangle|J\Omega M\rangle$.

The perturbation at long internuclear distance, where the electronic states are expressed by Hund's case c, can occur mostly by the S-uncoupling interaction H_{JS} or the L-uncoupling interaction H_{JL}. Nonvanishing matrix elements of the S-uncoupling interaction for the wave functions given by eqs 1−4 are

$$\langle ^3\Pi_2 \pm vJM|H_{JS}|^3\Pi_1 \pm v'JM\rangle = -\langle v|B|v'\rangle\sqrt{2(J+2)(J-1)}$$

$$\langle ^3\Pi_0 \pm vJM|H_{JS}|^3\Pi_1 \pm v'JM\rangle = -\langle v|B|v'\rangle\sqrt{2J(J+1)}$$

$$\langle ^3\Sigma^+_1 + vJM|H_{JS}|^3\Sigma^+_{0^-}v'JM\rangle = -\langle v|B|v'\rangle 2\sqrt{J(J+1)} \quad (5)$$

where $B = h^2/8\pi^2\mu R^2$, h is Planck's constant, μ is the reduced mass, and R is the internuclear distance.

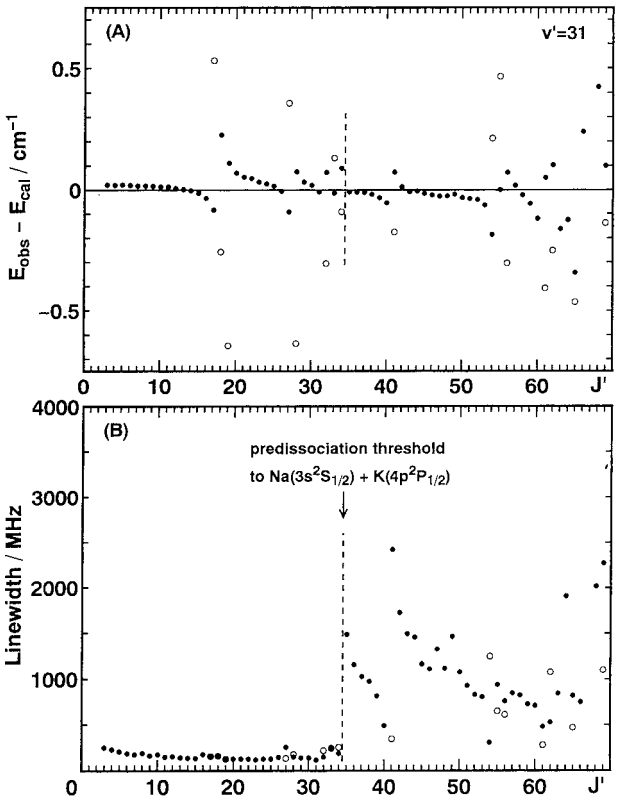

Figure 3. (A) Difference between the observed term value E_{obs} of the $B^1\Pi(v' = 31, J'e)$ level and the energy E_{cal} calculated from the molecular constants in Table 1 plotted against J' by a filled circle. That of the perturbing level is plotted by an open circle. (B) The observed line width of the $B^1\Pi(v' = 31, J'e) \leftarrow X^1\Sigma^+(v'' = 2, J' \pm 1e)$ transition is plotted against J' by a filled circle. That of the transition to the perturbing level is plotted by an open circle. The predissociation threshold is indicated by a broken line. Those of the $B^1\Pi(v' = 31, J'f)$ levels are similar.

Nonvanishing matrix elements of the L-uncoupling interaction for the wave functions given by eqs 1−4 are

$$\langle {}^3\Pi_2 \pm vJM|H_{JL}|{}^3\Sigma_1^+ \pm v'JM\rangle = -\langle v|B|v'\rangle\langle +1|L_+|0^+\rangle\sqrt{(J+2)(J-1)}$$

$$\langle {}^3\Pi_1 + vJM|H_{JL}|{}^3\Sigma_{0^-}^+ v'JM\rangle = -\langle v|B|v'\rangle\langle +1|L_+|0^+\rangle\sqrt{2J(J+1)}$$

$$\langle {}^3\Pi_0 \pm vJM|H_{JL}|{}^3\Sigma_1^+ \pm v'JM\rangle = \mp\langle v|B|v'\rangle\langle +1|L_+|0^+\rangle\sqrt{J(J+1)}$$

$$\langle {}^1\Pi + vJM|H_{JL}|{}^1\Sigma_{0^+}^+ v'JM\rangle = -\langle v|B|v'\rangle\langle +1|L_+|0^+\rangle\sqrt{2J(J+1)} \quad (6)$$

where the relation $\langle +1|L_+|0^+\rangle = \langle -1|L_-|0^+\rangle$ is used.

A. Predissociation to the Na(3s^{2}S$_{1/2}$) + K(4p^{2}P$_{1/2}$) Atoms. The difference between the observed term value E_{obs} of the $B^1\Pi(v' = 31, J')$ level and the energy E_{cal} calculated from the molecular constants in Table 1 is plotted against J' in Figure 3A. The magnitude of the perturbation can be seen as the deviation from zero, and the perturbing levels can be identified as the ones of a bound state. The observed line width of the $B^1\Pi(v' = 31, J') \leftarrow X^1\Sigma^+(v'' = 2, J' \pm 1)$ transition is plotted against J' in Figure 3B. The line width broadens abruptly at $J' \geq 35$, and it changes drastically centered at $J' = 41$, 54, and $J' > 60$, where large energy shifts are observed. Line broadenings are also observed for transitions to the $B^1\Pi(v' = 30, J' \geq 42)$, $(v' = 32, J' \geq 27)$, $(v' = 33, J' \geq 14)$, and $(v' \geq 34$, all $J')$ levels. The $E_{obs} - E_{cal}$ value for the $B^1\Pi(v' = 33, J')$ level is plotted against J' in Figure 4A, and the line width of the $B^1\Pi(v' = 33, J') \leftarrow X^1\Sigma^+(v'' = 2, J' \pm 1)$ transition is plotted against J' in Figure 4B. The term values of the $B^1\Pi(v' = 30, J' = 42)$, $B^1\Pi(v' = 31, J' = 35)$, $B^1\Pi(v' = 32, J' = 27)$, and $B^1\Pi(v' = 33, J' = 14)$ levels are, respectively, 18 263.8927, 18 262.2249, 18 261.3186, and 18 259.1568 cm^{-1}, which are marked by open circles in Figure 2.

The dissociation energy D_e of the $X^1\Sigma^+$ state is calculated to be 5273.716 ± 0.019 cm^{-1} from the data of Ishikawa et al.[14] By adding the 12 985.17 cm^{-1} energy of the K(4p^{2}P$_{1/2}$) level to the dissociation energy of the $X^1\Sigma^+$ state, the dissociation limit to the Na(3s^{2}S$_{1/2}$) + K(4p^{2}P$_{1/2}$) atoms is calculated to be 18 258.89 ± 0.02 cm^{-1}. The line broadenings above the dissociation limit are identified as originating from the predissociation to the Na(3s^{2}S$_{1/2}$) + K(4p^{2}P$_{1/2}$) atoms, which is caused by the spin−orbit interaction H_{SO} between the $B^1\Pi$ and $c^3\Sigma^+$ states.[2] Nonvanishing matrix elements of H_{SO} between $^1\Pi$ and $^3\Sigma^+$ states are[13]

$$\langle {}^3\Sigma^+ v_c N = JJM|H_{SO}|{}^1\Pi + v'JM\rangle = C_1\langle v_c|v'\rangle$$

$$\langle {}^3\Sigma^+ v_c N = J+1JM|H_{SO}|{}^1\Pi - v'JM\rangle = C_1\langle v_c|v'\rangle[J/(2J+1)]^{1/2}$$

$$\langle {}^3\Sigma^+ v_c N = J-1JM|H_{SO}|{}^1\Pi - v'JM\rangle = C_1\langle v_c|v'\rangle[(J+1)/(2J+1)]^{1/2} \quad (7)$$

where C_1 is a constant, $\langle v_c|v'\rangle$ is the overlap integral of the vibrational wave functions, and $|{}^3\Sigma^+ v_c N = J$ or $J \pm 1JM\rangle$ is the basis function in Hund's case b.

The effective potential energy for the rotating molecule of the rotational quantum number J is given by[15]

$$V_J(R) = V_0(R) + \frac{h^2}{8\pi^2\mu R^2}J(J+1) \quad (8)$$

where $V_0(R)$ is the potential energy for the nonrotating molecule. The effective potential curve has the potential barrier, and the energy of the last quasibound stable rotational level decreases with increasing v.[15] This is coincident with the observed results: the last stable levels are $J' = 41$ for $v' = 30$, $J' = 34$ for $v' = 31$, $J' = 26$ for $v' = 32$, and $J' = 13$ for $v' = 33$, and the term values decrease with v' as shown in Figure 2. Therefore, the observed (v', J') dependence of the threshold of the line broadening (predissociation threshold) can be attributed to the potential barrier due to rotation.

B. Perturbations below the Predissociation Threshold. A rotational perturbation, where several successive rotational lines deviate from the normal position centered at a certain J' (we shall call the J' level with maximum deviation the perturbation center), appears for a perturbation between bound states. Below and near the predissociation threshold, a series of perturbation centers which converge to the predissociation threshold of the Na(3s^{2}S$_{1/2}$) + K(4p^{2}P$_{1/2}$) atoms is observed for each v', and these are shown by open squares in Figure 2. Transition lines to the perturbing levels are also observed. By subtracting the energy shift due to the perturbation with the $B^1\Pi(v', J')$ level, the line positions of the perturbing levels in the absence of perturbation are evaluated. The rotational constant $B_v = \langle v|B|v\rangle$ is determined to be 0.015 cm^{-1} for levels perturbing the $B^1\Pi(v' = 31, J' = 17-19)$ levels. Only the $c^3\Sigma^+$ and $A^1\Sigma^+$ states are correlated adiabatically with the separated atoms Na(3s^{2}S$_{1/2}$)

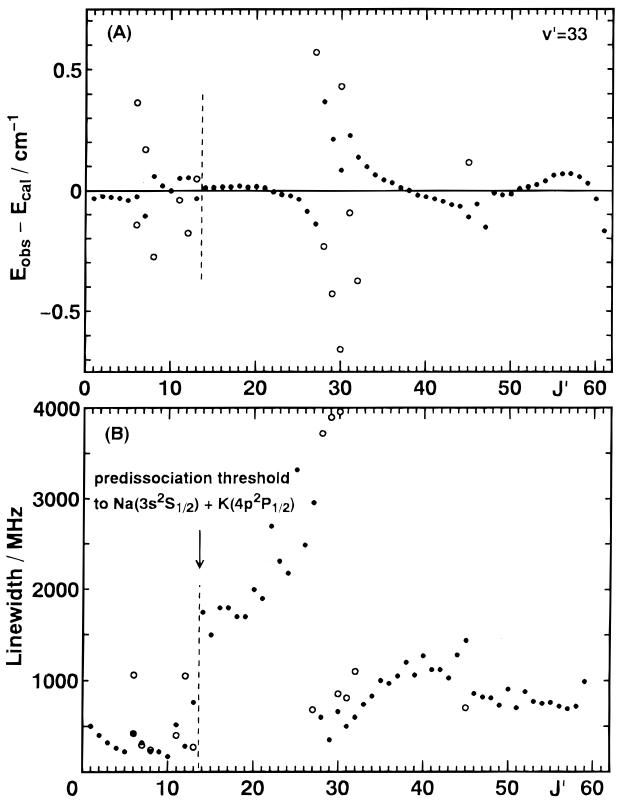

Figure 4. (A) Difference $E_{obs} - E_{cal}$ of the $B^1\Pi(v' = 33, J'e)$ level plotted against J' by a filled circle. That of the perturbing level is plotted by an open circle. (B) The observed line width of the $B^1\Pi(v' = 33, J'e) \leftarrow X^1\Sigma^+(v'' = 2, J' \pm 1e)$ transition is plotted against J' by a filled circle. That of the transition to the perturbing level is plotted by an open circle. Those of the $B^1\Pi(v' = 33, J'f)$ levels are similar.

$+ K(4p^2P_{1/2})$, and only the $c^3\Sigma^+$ state can interact with the $B^1\Pi$ state by the spin−orbit interaction. Therefore, the perturbing state can be identified as the $c^3\Sigma^+$ state.

For the transition lines to the strongly perturbed $B^1\Pi(v' = 32, J' = 10-28)$ levels, the hyperfine structures are observed for the f-components but are not observed for the e-components. The hyperfine splitting of the $^3\Sigma^+$ state was shown to be small for the e-component and large for the f-component.[16] Only the e (f)-component of the $^1\Pi$ state can interact with the e (f)-component of the $^3\Sigma^+$ state by the spin−orbit interaction. Mixing of the $^1\Pi$ and $^3\Sigma^+$ states by the perturbation can make the hyperfine structure appreciable in the $^1\Pi$(f-component) level but not in the $^1\Pi$(e-component) level. This is consistent with the identification that the perturbing state is the $c^3\Sigma^+$ state.

C. Perturbation above the Predissociation Threshold. Above the dissociation limit to the $Na(3s^2S_{1/2}) + K(4p^2P_{1/2})$ atoms, the predissociation of the $B^1\Pi$ state is observed as line broadening. In addition to this, rotational perturbations are observed. The bound state which can perturb the $B^1\Pi$ state is the $b^3\Pi$ state, which splits into 2, 1, 0^+, and 0^- states at long internuclear distance $R > 8$ Å. The perturbation between the $B^1\Pi$ and $b^3\Pi$ states occurs by the spin−orbit interaction. Nonvanishing matrix elements of H_{SO} between $^1\Pi$ and $^3\Pi$ states are[13]

$$\langle {}^3\Pi_1 - vJM|H_{SO}|{}^1\Pi + v'JM\rangle = -\zeta\langle v|v'\rangle$$

$$\langle {}^3\Pi_1 + vJM|H_{SO}|{}^1\Pi - v'JM\rangle = -\zeta\langle v|v'\rangle \quad (9)$$

where ζ is a constant. Therefore, the perturbing state is the $b^3\Pi_1$ state.

It is interesting to note that the line widths are observed to change drastically around the perturbation center. For example, the perturbation center is observed at $J' = 41$ for the $B^1\Pi(v' = 31, J')$ levels (see Figure 3A). The line width is observed to decrease as J' approaches 40 from below; it suddenly becomes a maximum at $J' = 41$ and decreases gradually as J' exceeds 41 (see Figure 3B). Another perturbation center is observed at $J' = 28$ for the $B^1\Pi(v' = 33, J')$ levels (see Figure 4A). The line width is observed to increase as J' approaches 27 from below, and it suddenly becomes very small at $J' = 28$ and increases gradually as J' exceeds 28 (see Figure 4B). Let us further consider these phenomena.

The eigenvalue and the eigenfunction of the $B^1\Pi(v', J')$ level perturbed by the $b^3\Pi_1(v, J')$ level are given by

$$E_1 = (1/2)[H_{11} + H_{22} \langle\pm\rangle \sqrt{(H_{11} - H_{22})^2 + 4H_{12}{}^2}] \quad (10)$$

$$\Phi_1 = N^{-1/2}\{[H_{11} - H_{22} \langle\pm\rangle \sqrt{(H_{11} - H_{22})^2 + 4H_{12}{}^2}]\phi_1 + 2H_{12}\phi_2\} \quad (11)$$

where ϕ_1 and ϕ_2 are, respectively, the wave functions of the unperturbed $B^1\Pi(v', J')$ and $b^3\Pi_1(v, J')$ levels, H_{11} and H_{22} are the energies of the unperturbed levels, H_{12} is the matrix element of the perturbation, $\langle\pm\rangle$ is + for $H_{11} > H_{22}$ and − for $H_{11} < H_{22}$, and $N = 4H_{12}{}^2 + [H_{11} - H_{22} \langle\pm\rangle \sqrt{(H_{11}-H_{22})^2+4H_{12}{}^2}]^2$. Nonvanishing matrix elements of H_{SO} between $^3\Sigma^+$ and $^3\Pi_1$ states are[13]

$$\langle {}^3\Sigma^+ v_c N = JJM|H_{SO}|{}^3\Pi_1 - vJM\rangle = C_2\langle v_c|v\rangle$$

$$\langle {}^3\Sigma^+ v_c N = J + 1JM|H_{SO}|{}^3\Pi_1 + vJM\rangle = C_2\langle v_c|v\rangle[J/(2J+1)]^{1/2}$$

$$\langle {}^3\Sigma^+ v_c N = J - 1JM|H_{SO}|{}^3\Pi_1 + vJM\rangle = C_2\langle v_c|v\rangle[(J+1)/(2J+1)]^{1/2} \quad (12)$$

where C_2 is a constant. Both the $B^1\Pi(v', J')$ and $b^3\Pi_1(v, J')$ states can interact with the $c^3\Sigma^+$ state through spin−orbit coupling.

From eqs 7, 11, and 12, nonvanishing matrix elements of $\langle c^3\Sigma^+|H_{SO}|\Phi_1\rangle$ are

$$\langle c^3\Sigma^+ v_c N = JJM|H_{SO}|\Phi_1(B^1\Pi + v'JM)\rangle = N^{-1/2}\{[H_{11} - H_{22} \langle\pm\rangle \sqrt{(H_{11} - H_{22})^2 + 4H_{12}{}^2}]C_1\langle v_c|v'\rangle + 2H_{12}C_2\langle v_c|v\rangle\}$$

$$\langle c^3\Sigma^+ v_c N = J + 1JM|H_{SO}|\Phi_1(B^1\Pi - v'JM)\rangle = N^{-1/2}\{[H_{11} - H_{22} \langle\pm\rangle \sqrt{(H_{11} - H_{22})^2 + 4H_{12}{}^2}]C_1\langle v_c|v'\rangle \times [J/(2J+1)]^{1/2} + 2H_{12}C_2\langle v_c|v\rangle[J/(2J+1)]^{1/2}\}$$

$$\langle c^3\Sigma^+ v_c N = J - 1JM|H_{SO}|\Phi_1(B^1\Pi - v'JM)\rangle = N^{-1/2}\{[H_{11} - H_{22} \langle\pm\rangle \sqrt{(H_{11} - H_{22})^2 + 4H_{12}{}^2}]C_1\langle v_c|v'\rangle \times [(J+1)/(2J+1)]^{1/2} + 2H_{12}C_2\langle v_c|v\rangle[(J+1)/(2J+1)]^{1/2}\} \quad (13)$$

In the region of perturbation between the $B^1\Pi(v', J')$ and $b^3\Pi_1(v, J')$ levels, the overlap integral $\langle v'|v\rangle$ of the vibrational wave functions is of appreciable magnitude, and thus both vibrational wave functions $|v'\rangle$ and $|v\rangle$ can have overlap integrals of

appreciable magnitude with the vibrational wave function $|v_c\rangle$ of the dissociative continuum of the $c^3\Sigma^+$ state.

The rate of predissociation, hence the line width, of the perturbed level is proportional to $|\langle c^3\Sigma^+|H_{SO}|\Phi_1\rangle|^2$. If H_{12} is negative, the coefficients of ϕ_1 and ϕ_2 in the eigenfunction Φ_1 of eq 11 are of the same sign on the low-energy side of the perturbation center (in the region $H_{11} < H_{22}$). Then, the perturbation between $c^3\Sigma^+$ and ϕ_1 and the perturbation between $c^3\Sigma^+$ and ϕ_2 contribute constructively to the predissociation rate. The predissociation rate will increase as J' approaches the perturbation center from the low-energy side. Above the perturbation center (in the region $H_{11} > H_{22}$), the coefficients of ϕ_1 and ϕ_2 become of opposite signs. Then, the perturbation between $c^3\Sigma^+$ and ϕ_1 and the one between $c^3\Sigma^+$ and ϕ_2 contribute destructively to the predissociation rate. The predissociation rate abruptly becomes very small just above the perturbation center and it gradually increases toward higher energy. This is the case of $v' = 33$, $J' = 15-40$ (see Figure 4). If H_{12} is positive, the coefficients of ϕ_1 and ϕ_2 in the eigenfunction Φ_1 of eq 11 are of different signs on the low-energy side of the perturbation center. The perturbation between $c^3\Sigma^+$ and ϕ_1 and the one between $c^3\Sigma^+$ and ϕ_2 contribute destructively and the predissociation rate decreases as J' approaches the perturbation center from the low-energy side. Above the perturbation center, the perturbation between $c^3\Sigma^+$ and ϕ_1 and the one between $c^3\Sigma^+$ and ϕ_2 contribute constructively. The predissociation rate will abruptly become a maximum just above the perturbation center, and it will gradually decrease on the high-energy side. This is the case of $v' = 31$, $J' = 35-50$ (see Figure 3). The sign of H_{12} changes by the sign of the overlap integral $\langle v'|v\rangle$. The observed drastic change of the line width around the perturbation center can be explained by this interference effect.

At $v' = 33$, $J' = 30$, three lines of the same J' are observed (see Figure 4A). The $^3\Pi$ state is composed of $^3\Pi_2$, $^3\Pi_1$, and $^3\Pi_0$, and the eigenfunctions of the perturbing levels can be a mixture. The mixed components can interact with the $B^1\Pi$ state by H_{SO}, and as a result three lines for a given J' may be allowed.

D. Perturbation near the Dissociation Threshold. By adding the 13 042.89 cm^{-1} energy of the $K(4p^2P_{3/2})$ level to the dissociation energy 5273.716 ± 0.019 cm^{-1} of the $X^1\Sigma^+$ state, the dissociation limit to the $Na(3s^2S_{1/2}) + K(4p^2P_{3/2})$ atoms is calculated to be 18 316.61 ± 0.02 cm^{-1}. Therefore, there should be transition lines up to $v' = 44$ (small J) as we can estimate from the plots of Figure 2. However, we could not identify those with confidence because the intensity became weak and the signal became comparable with noise. A number of transitions to levels above the dissociation limit are observed. The rotational levels separated from the dissociative state by a potential barrier due to rotation are metastable. Dissociation through the tunneling effect, which is called rotational predissociation, can occur below the maximum of the effective potential curve and the transition line to such a level may be broad and weak. Therefore, the true breaking-off point must lie above the highest observed rotational level in each vibrational level. The highest rotational levels are observed to decrease both in energy and J' as v' increases (see Figure 2). The energy difference between the highest observed rotational levels $B^1\Pi(v_a, J_a)$ and $B^1\Pi(v_b, J_b)$ for $v_a \neq v_b$ is given by[15]

$$E(v_a,J_a) - E(v_b,J_b) = \frac{h^2}{8\pi^2\mu R^2}[J_a(J_a+1) - J_b(J_b+1)] \quad (14)$$

where the potential maxima for J_a and J_b are assumed to lie at about the same R value, which holds if J_a is close to J_b. If we could observe the rotational levels up to the breaking-off point, we would be able to calculate the energy and internuclear distance of the potential maximum. The highest rotational levels are $J' = 58$ for $v' = 34$ and $J' = 55$ for $v' = 35$, and the level energies are, respectively, 18 333.3938 and 18 330.9074 cm^{-1}. Using eq 14, the potential maximum is calculated to lie at $R =$ 12.7 Å for $J' = 55-58$. The highest rotational levels are $J' =$ 49 for $v' = 36$ and $J' = 45$ for $v' = 37$, and the level energies are, respectively, 18 326.0361 and 18 324.0534 cm^{-1}. Then, the potential maximum is calculated to lie at $R = 14.9$ Å for J' $= 45-49$. The potential maximum moves to smaller R as J' increases. The line width is observed to increase as the highest rotational level is approached. The line shape is observed to be non-Lorentzian, and it contains the hyperfine splitting. Therefore, it is not possible to evaluate the rate of the rotational predissociation from the line width.

In the transitions to high vibrational levels ($v' \geq 37$), two lines are observed for each J' (see Figure 2), in which one is strong and the other is weak. The weak component is considered to have been allowed by the perturbation at long internuclear distance, and therefore it is appropriate to discuss in Hund's case c basis. The perturbation between the 1(a) and 2 states, whose potential curves are very close at $R > 10$ Å (see Figure 1B), may be the cause of the line splitting. The eigenfunction of the 1(a) state is a mixture of the basis functions $|^1\Pi\rangle$ and $|^3\Pi_1\rangle$.[2] The perturbation between the 1(a) and 2 states can occur by the *S*-uncoupling interaction (see eq 5), and the magnitude is proportional to $\langle v|B|v'\rangle\sqrt{2(J+2)(J-1)}$. The magnitude of $\langle v|B|v'\rangle$ may be insensitive to J at high v', because the vibrational wave functions can overlap constructively at long internuclear distance and the effect of rotation is small at large R. The *S*-uncoupling interaction is expected to become strong as J increases; this is consistent with the observed result that the line splitting increases with J. The reasons why the line splittings are observed for almost all J' will be that the energy spacing between the vibrational levels $B^1\Pi[1(a)](v')$ and $b^3\Pi$-$[2](v)$ is small at high $v' \geq 37$ and the perturbation occurs at long internuclear distance.

E. Line Splitting of the $B^1\Pi(v' = 30, J')$ Level. The line splittings of the $B^1\Pi(v' = 30, J')$ levels are different from the ones of the $v' = 31-36$ levels. The splitting is observed for almost all J', and the magnitude of splitting increases with J' (see Figure 2). We have confirmed that such a splitting is not observed for $v' = 29$ by choosing several J' levels. Since the splitting is observed for both above and below the predissociation threshold, the perturbing state must be a state correlated with the separated atoms $Na(3s^2S_{1/2}) + K(4p^2P_{3/2})$. The perturbation is presumed to occur at long internuclear distance because the splitting is observed for almost all J'. It can occur by the *S*-uncoupling interaction, and the perturbing state is either the 2 state or the $0^{\pm}$ (a) state as we can see from eq 5. The hyperfine structures are observed in both of the split lines, and some of those are shown in Figure 5. Such hyperfine structures are observed for both the e- and f-components.

The de Broglie wavelength λ, from which we can make a rough estimate of the wavelength of the vibrational wave function at a given kinetic energy, for the kinetic energy K is given by

$$\lambda = h(2\mu K)^{-1/2} \quad (15)$$

where μ is the reduced mass of $^{23}Na^{39}K$. At $K = 50$ cm^{-1}, λ is calculated to be 0.96 Å for $^{23}Na^{39}K$. The overlap integral $\langle v|v'\rangle$ between the vibrational wave functions of the 2 and 1(a) states at a given energy E is expected to be large for $v' \geq 30$, because the vibrational wave functions around the outer turning

points are expected to overlap constructively. On the other hand, the overlap integral $\langle v|v'\rangle$ of the vibrational wave functions of the $0^{\pm}$ (a) and 1(a) states around $E = 18\ 220\ cm^{-1}$ is presumed to be small, because the vibrational wave functions around the outer turning points are expected to overlap destructively because the wavelengths of the two vibrational wave functions are different at the overlapping region. Therefore, the perturbing state is presumed to be the 2 state.

In order to have a significant mixing, the energy difference between the two perturbing levels must be smaller than the perturbation energy. Therefore, it is presumed that the energy of the $B^1\Pi[1(a)](v' = 30)$ level is accidentally coincident with the one of $2(v)$ level. The energies of the $B^1\Pi[1(a)](v' = 31-36)$ levels are probably not coincident with those of $2(v)$ levels, and this may be the reason why line splittings, similar to the ones observed for the $B^1\Pi[1(a)](v' = 30, J')$ levels, are not observed in these levels.

Nonvanishing matrix elements of the hyperfine interaction due to the magnetic dipole interaction $H_{MD}(1)$ with the nuclear spin $\mathbf{I}_1$ in the $^3\Pi$ state are given by[13]

$$\langle {}^3\Pi_1 \pm vJI_1F_1M_{F_1}|H_{MD}(1)|{}^3\Pi_1 \pm vJI_1F_1M_{F_1}\rangle = [F_1JI_1]\frac{1}{4J(J+1)}G(1)$$

$$\langle {}^3\Pi_2 \pm vJI_1F_1M_{F_1}|H_{MD}(1)|{}^3\Pi_2 \pm vJI_1F_1M_{F_1}\rangle = [F_1JI_1]\left[\frac{1}{2\sqrt{2}J(J+1)}K(1) + \frac{1}{2J(J+1)}G(1) + \frac{1}{\sqrt{2}J(J+1)}D(1;1+1)\right]$$

$$\langle {}^3\Pi_0 \pm vJI_1F_1M_{F_1}|H_{MD}(1)|{}^3\Pi_1 \pm vJI_1F_1M_{F_1}\rangle = [F_1JI_1]\frac{1}{8\sqrt{J(J+1)}}[K(1) - D(1;1+1) \pm \sqrt{6}D(1;1-1)]$$

$$\langle {}^3\Pi_1 \pm vJI_1F_1M_{F_1}|H_{MD}(1)|{}^3\Pi_2 \pm vJI_1F_1M_{F_1}\rangle = [F_1JI_1]\frac{\sqrt{(J-1)(J+2)}}{8J(J+1)}[K(1) - D(1;1+1)] \quad (16)$$

where $[F_1JI_1] = F_1(F_1+1) - J(J+1) - I_1(I_1+1)$. $K(1)$, $G(1)$, and $D(1;1 \pm 1)$ are constants which arise, respectively, from the Fermi contact interaction, the nuclear spin−electron orbital angular momentum interaction, and the nuclear spin−electron spin dipole interaction. The nuclear spins of ^{23}Na and ^{39}K atoms are both 3/2. The quantum number F_1 of the total angular momentum takes $J + 3/2$, $J + 1/2$, $J - 1/2$, and $J - 3/2$ for a given J. Therefore, the splitting into four lines (see Figure 5) can be identified as the hyperfine splitting. This splitting may be originating mainly from the Fermi contact interaction with the nucleus of ^{23}Na, because the $b^3\Pi$ state is correlated with the separated atoms $Na(3s^2S_{1/2}) + K(4p^2P_{3/2})$.

The diagonal matrix elements are proportional to J^{-1} for large J, and become small as J increases. If the $^3\Pi_1$ and $^3\Pi_2$ states are mixed, as is caused by the S-uncoupling interaction, the matrix element $\langle {}^3\Pi_1 \pm vJI_1F_1M_{F_1}|H_{MD}(1)|{}^3\Pi_2 \pm vJI_1F_1M_{F_1}\rangle$ gives the main contribution. The wave functions $|{}^3\Pi+\rangle$ and $|{}^3\Pi-\rangle$ are, respectively, the f- and e-components. The magnitude becomes constant at large J, and hyperfine splitting is expected to occur both for the e- and f-components. These are coincident with the observed results. We conclude that the $B^1\Pi$-[1(a)]($v' = 30$) and $2(v)$ levels are accidentally coincident in energy and the line splitting is caused by the S-uncoupling interaction between these levels at a long internuclear distance.

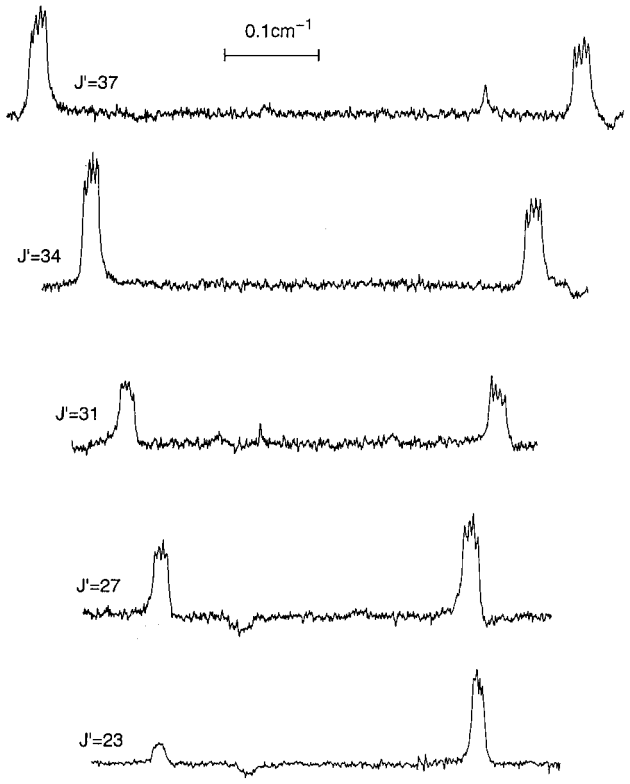

Figure 5. Some of the observed OODRPS spectra of the split lines of the $B^1\Pi(v' = 30, J'e) \leftarrow X^1\Sigma^+(v'' = 2, J' - 1e)$ transitions.

Conclusions

OODRPS technique has been used to examine the v' and J' dependencies of energy and line width of the $^{23}Na^{39}K$ $B^1\Pi \leftarrow X^1\Sigma^+$ transitions up to the breaking-off points, where NaK dissociates to the $Na(3s^2S_{1/2}) + K(4p^2P_{3/2})$ atoms. OODRPS is a very powerful method which enables us to observe transitions from a selected level at high resolution and high sensitivity. Line broadenings are observed for transitions to the $B^1\Pi(v' = 30, J' \geq 42)$, $(v' = 31, J' \geq 35)$, $(v' = 32, J' \geq 27)$, $(v' = 33, J' \geq 14)$, and $(v' \geq 34$, all $J')$ levels, and are attributed to the predissociation via the $c^3\Sigma^+$ state to the $Na(3s^2S_{1/2}) + K(4p^2P_{1/2})$ atoms. Rotational perturbations are observed above the predissociation threshold, and the perturbing state is identified as the $b^3\Pi_1$ state. The line widths are observed to change drastically around the perturbation center, and this is identified as originating from the interference effect which arises because both the $B^1\Pi$ and $b^3\Pi_1$ states interact with the dissociative continuum of the $c^3\Sigma^+$ state.

When optical transitions from an initial state to both a discrete level and the continuum are allowed, an interference effect depending on the relative signs of transition moments is observed as an asymmetric line broadening, which is called Fano profile.[17] The interference effect found in this work is another kind of interference in predissociation. When two bound states are mixed by perturbation and both the bound basis states interact with a dissociative continuum, the interference effect in predissociation appears. In the case that an optical transition is allowed to only one of the bound basis states, this effect can be observed as a drastic change of the line widths around the perturbation center between the bound states. Such an interference effect is universal, and it would be important for further understanding of chemical reactions. The present work is the first finding of this phenomenon as far as the authors know.

In the transitions to levels near the breaking-off points of the $B^1\Pi(v' \geq 37)$, the line splittings into two lines are observed for each J'. This splitting is identified as originating from the *S*-uncoupling interaction between the $B^1\Pi[1(a)]$ and $b^3\Pi[2]$ states at a long internuclear distance. Similar line splittings are observed for the $B^1\Pi(v' = 30$, all $J')$ levels, but are not observed for $v' = 31-36$. An accidental coincidence of the level energies of the $B^1\Pi[1(a)](v' = 30)$ and $b^3\Pi[2](v)$ levels is presumed, and the origin of the line splitting is also identified as the *S*-uncoupling interaction at a long internuclear distance. Below the predissociation threshold, a series of the perturbation centers which converge to the threshold is observed for each v', and the perturbing state is identified as the $c^3\Sigma^+$ state. Such interactions can occur in general, especially near the dissociation limit of an excited state, and can now be observed by using techniques of multiple resonance laser spectroscopy.

Acknowledgment. This work is supported by a grant in aid for specially promoted research from the Ministry of Education, Science and Culture of Japan. H.K. is very grateful to Professor S. Nagakura for his encouragement and support.

References and Notes

(1) Moore, C. E. *Atomic Energy Levels. Vols. 1−3*; National Bureau of Standards (U.S.) No. 467; U.S. GPO: Washington, DC, 1971.

(2) Kasahara, S.; Baba, M.; Katô, H. *J. Chem. Phys.* **1991**, *94*, 7713.

(3) Teets, R. E.; Kowalski, F. V.; Hill, W. T.; Carlson, N.; Hänsch, T. W. *SPIE J.* **1977**, *113*, 80.

(4) Carlson, N. W.; Taylor, A. J.; Jones, K. M.; Schawlow, A. L. *Phys. Rev. A* **1981**, *24*, 822.

(5) Raab, M.; Höning, G.; Demtröder, W.; Vidal, C. R. *J. Chem. Phys.* **1982**, *76*, 4370.

(6) Ross, A. J.; Clements, R. M.; Barrow, R. F. *J. Mol. Spectrosc.* **1988**, *127*, 546.

(7) Ross, A. J.; Effantin, C.; d'Incan, J.; Barrow, R. F. *J. Phys. B* **1986**, *19*, 1449.

(8) Kowalczyk, P.; Sadeghi, N. *J. Chem. Phys.* **1995**, *102*, 8321.

(9) Rydberg, R. *Z. Phys.* **1931**, *73*, 376. Klein, O. *Z. Phys.* **1932**, *76*, 226. Rees, A. L. G. *Proc. Phys. Soc. London* **1947**, *A59*, 998.

(10) Zare, R. N. *J. Chem. Phys.* **1964**, *40*, 1934.

(11) Ikoma, H.; Kasahara, S.; Katô, H. *Mol. Phys.* **1995**, *85*, 799.

(12) Ross, A. J.; Effantin, C.; d'Incan, J.; Barrow, R. F. *Mol. Phys.* **1985**, *56*, 903.

(13) Katô, H. *Bull. Chem. Soc. Jpn.* **1993**, *66*, 3203.

(14) Ishikawa, K.; Mukai, N.; Tanimura, M. *J. Chem. Phys.* **1994**, *101*, 876.

(15) Herzberg, G. *Molecular Spectra and Molecular Structure. I. Spectra of Diatomic Molecules*; Van Nostrand Reinhold: New York, 1950.

(16) Ishikawa, K.; Kumauchi, T.; Baba, M.; Katô, H. *J. Chem. Phys.* **1992**, *96*, 6423.

(17) Lefebvre-Brion, H.; Field, R. W. *Perturbations in the Spectra of Diatomic Molecules*; Academic: Orlando, 1986.